We thank the referee for his/her time to provide us with extensive and valuable input. Please find below our responses to the raised comments, questions and suggestions. In the following, raised **comments / suggestions are in red** and respective **responses in green**, while **alterations to the manuscript text are indicated in blue.**

General Comment

This manuscript presented a detailed analysis of a large data set of size-resolved particle composition measured by HR-AMS in Hong Kong. Both long-term trends and diurnal variations of the mass size distributions of submicron organic material, sulfate, and nitrate are discussed on the basis of previous understanding about the sources. Variations in the particle mixing state are also evaluated. This is perhaps the first study that looked at long-term AMS mass size distributions systematically, which potentially may serve as a good example of utilizing such data to derive better understanding of the sources and the atmospheric processing of submicron particles. The current manuscript has however not yet arrived there. My main suggestions are (1) to justify the possible bias of the deconvolution of the mass size distributions (Bian et al., 2014) maybe exclude some data; see my comment #1) and (2) to make a clear difference on which results are novel and which ones have already been published from previous analysis. Also, some figures contain too much information and hence are difficult to read. I therefore think a major revision or a resubmission is needed before this paper being accepted as a publication on ACP.

We provide a discussion with respect to (1) and (2) further below in the specific comment section. In terms of figure complexity, we understand that the provided information density per figure is high. We are thus providing a revised set of figures. The main data presented in this work have not been published before, but are based on further in-depth analysis of ambient datasets which have been discussed previously.

Specific Comments

Comment   (1) As shown in Figure D1, Aitken-mode peak often occurred in the left tail of the Accumulation-mode peak. If the heights of the two peak differ a lot (for example, one as only a few percent of the other one), it is easy to overfit the small peak, which may cause large uncertainties in quantifying the small peak. It is unclear to me how such overfitting is controlled in this study. Are any of the data points in Figures 1, 2, and 5 subject to this possibility?

Response   In the vast majority of analyzed size distributions the bimodal characteristics were very obvious, and unimodal fitting of such distributions would lead to large positive residuals in the lower size region, justifying the fitting of a second peak.

In extreme cases, as the reviewer notes, the difference in peak height (and peak area) between the two fitted modes can be large. When the ratio of Aitken to accumulation mode was very small (<10%), we evaluated both uni- and bimodal peak fits for which we depict one example such an extreme case below (Figure R1). In this case, from the day-to-day size distribution set (suburban HKUST site, fall, SO4), the peak area ratio of Aitken to accumulation mode was ~2%. The lognormal peak fittings are presented in subpanel (a) for the unimodal case and (b) for the bimodal case. Panels (c) and (d) show histograms of the residuals from both cases. Panel (e) shows the cumulative probability distribution for the residuals from both fittings and the calculated D value from the Kolmogorov-Smirnov Test at 95% CI. It is obvious that even in such an extreme case, the bimodal fitting resolve the raw distribution more accurately with a quasi-normal residual distribution and cumulative probability density function. In contrast, the unimodal fitting exhibits a considerably skewed residual distribution that is tail-heavy towards larger positive concentration values and centered towards negative residuals. We obtained similar results for all borderline cases in our measurements and thus generally opted for bimodal deconvolution. We are therefore confident that overfitting of the small peak was unlikely to be a major issue in this work, but we agree that this question is indeed relevant and we will include a more detailed discussion in the methodology sections of the main text and supplementary material for reference in the revised manuscript. The concerned discussion is appended at the bottom of this document.

With regard to the peak fit process itself, Igor's multipeak fitting tool uses the Levenberg-Marquardt algorithm to adjust the fit parameters with the goal to minimize the sum of squares of the deviations as an iterative process starting from the provided initial guesses. The standard deviations of the fit parameters provide an estimate of the variability of parameters between the final fit solution and the surrounding solution space with similar, but slightly larger residuals. We provide a discussion of these analyses in the revised manuscript and Supporting Material.

Alteration	Revision and addition to Section B of the Supporting Material and associated Tables (C1-C3) and Figures (D2-D5). The relevant sections are appended at the bottom of this document.
Comment	(2) I disagree that the transmission efficiency of the AMS lens unlikely affects the presented analysis (Line 122-126). Because the particle velocity calibration only spans for a certain range, extrapolation of fit may lead overestimation of the mass size distributions in small sizes. Slow vaporization and bounce may lead overestimation at $D_{va} > 1$ µm (Ref.: http://cires1.colorado.edu/jimenez-group/wiki/index.php / AMSUsrMtgs, Best Practices: IE and Velocity Calibrations - Ed Fortner & John Jayne). More importantly, the transmission efficiency for standard AMS lens drops at Dva> 400 nm or < 100 nm, and is below 20% for Dva > 1 µm or < 60 nm (Liu et al., 2007). The transmission therefore skews the size distributions. Zhang et al. (2005) showed that in Pittsburgh when the AMS suggests an accumulation mode at 500 nm, MOUDI shows a peak at 900 nm Dva. In this case, the fitting to AMS distributions might miss the main mode. Bian et al. (2014) showed that sulfate and nitrate etc. indeed occurred in mode size much greater than 500 nm Dva in Hong Kong. Given all the reasons, for urban area that has larger accumulation mode, I think the parameters (GSD, MMD, and integrated area) from fitting to the right peak (e.g., in Figure D1) cannot represent the actual accumulation-mode distributions. Ideally, the size distributions can be corrected for transmission efficiency (at least for the right side). But it is very difficult to obtain the transmission efficiency for a specific AMS with standard vaporizer. I suggest the authors to justify their accumulation-mode analysis by additional data (e.g., from SMPS or MOUDI) or improved algorithm. Otherwise, it may not be meaningful to discuss the accumulation-mode changes.
Response	We agree with the reviewer that lens transmission is an important issue in AMS-related work in general and represents a key instrumental limitation, which affects the vast majority of AMS publications as lens transmission corrections are not commonly performed.
	The main aim of our work however is to present an analysis method that can provide an additional dimension to standard AMS data analysis techniques, given that bi- or multimodal size distributions from AMS measurements have been reported frequently in the literature. In our study, we focus on discussing the trends of mode diameters and mode particle mass (peak area) to provide additional, complementing information to preceding studies that only utilized standard mass concentration based analyses.
	Lens transmission efficiencies have been reported to vary between instruments (even at the same pressure level) and a standard lens as used in this study is expected to transmit efficiently (~100%) between 90nm and 700nm D_{va}, thereafter decreasing to ~0.3 at 1000nm (Williams et al., 2013). The largest observed mode diameters in the accumulation mode in our work at either sampling location were ~700nm (D_{va}). The referenced size distribution work (Bian et al., 2014) relies on MOUDI samples and showed mode diameters ~800-900nm of aerodynamic diameter D_a, which if we assume $D_a \sim D_p$ and a particle density of ~ 1.5 g/cm^3 is beyond the transmission capability of the AMS (with $D_{va} \sim 1.4$ µm) in the droplet mode range. We note that comparability of results from MOUDI studies and AMS is limited given the different sizing techniques, sampling times (minute resolution vs. daily samples) and more importantly aerosol pretreatment i.e. "as-is" for MOUDI vs. removal of water prior to AMS measurements, which can influence particle size in high humidity (>80%) conditions (Fang et al., 1991).
	While we agree that additional particle sizing instrumentation for inter-instrumental comparison are useful, the measurements presented in this study were conducted with a limited set of available instruments and did unfortunately not encompass complementary particle size distribution measurements (by either electrostatic classification or MOUDI samplers).
	We revised the statements in line 122-126 and further stress the aims and scope of our work as well as the definition of the Aitken and accumulation mode as representing the apparent Aitken- and accumulation-mode contributions to AMS-measurable particle mass (i.e. within the capabilities and limitations of AMS as an ambient analytical instrument). We still view that the presented work is useful to the growing AMS community to offer additional dimensions in the analysis of AMS size distribution data.
Alteration	The transmission efficiency of the AMS aerodynamic lens is known to fall off beyond ~0.7 µm of vacuum-aerodynamic diameter (Liu et al., 2007;Takegawa et al., 2009;Zhang et al.,

2004;Bahreini et al., 2008;Williams et al., 2013) and may bias measured particle mass and mode diameters in the accumulation mode towards lower values if significant particle mass fractions fall in the size region of $D_{va} > 0.7$ µm. Resolved MMDs at either sampling location were typically within the efficient upper transmission limit in this work.

The discussion of size distributions in this work should be viewed in the context of the instrumental capabilities and limitations of aerosol mass spectrometry, i.e. resolved Aitken and accumulation modes in this work are understood to represent the apparent Aitken and accumulation modes within AMS measurable particle mass size distributions.

Comment   Figures 1 and 2: The discussions in page 5-11 are difficult to follow by reading those figures. For example, diurnal profiles for four gaseous pollutants have no size dependence. Showing them twice with the two particle modes is very confusing. Similarly, the shaded diurnal profiles for total submicron mass of different species made the figures difficult to read. I suggest to move those into a separate figure.

Response   Gas data are shown in duplicate (noted in the figure caption) to enable direct eye-guided comparison of concentration trends in both panels. We have revised the figures for more intuitive readability.

Alteration   Figures 1 and 2 (now Figures 2 and 3 in the revised manuscript) have been replotted.

Comment   The numbering of section 3.1, 3.2, and 3.2.1 seems wrong.

Response   The numbering of sections in chapter 3 is erroneous. Part 3.2. is in fact 3.1.1., while 3.2. is 3.1.2. This also affects section numbers thereafter, and we provide a corrected chapter numbering in the revised manuscript.

Comment   Line 157: "median values" - it is better to clarify in the captions of Figures 1 and 2 what are the medians.

Response   We state more clearly in the text and figure captions that median refers to values from the bin-median size distribution in the revised manuscript.

Comment   Line 161: What is "residual traffic"?

Response   We employ the term "residual traffic" in analogy to "background" concentration levels, as traffic in the central inner-city districts remains continuous at night albeit at much lower vehicle number compared to the daytime, whereas in more remote areas or smaller cities traffic at night is typically intermittent. We will change the wording to avoid confusion.

Alteration   […] as well as contributions from nighttime activity such as traffic, which remains continuous in the inner-city districts at night albeit at much lower vehicle numbers compared to the daytime.

Comment   Line 168: The abbreviations only need to be defined when the full terms first appear. Same in figure captions.

Response   We will remove duplicate definitions in the revised manuscript.

Comment   Line 191: What is "residual organic particle mass"?

Response   This term has been used in a context similar to the discussion of "residual traffic", and refers to any background organic aerosol contributions as well as local contributions that are not immediately removed by settling or sweep-out. We agree that this may be confusing.

Alteration   In the accumulation mode, organic particle mass during the night hours (00:00 – 06:00) was 2.5 times larger in spring (5.5 µg m^{-3}) than in summer (2.0 µg m^{-3}).

Comment   Line 186 and Line 215: Figures do not appear in order.

Response   In this manuscript, Figures have been arranged to enable the reader to compare the results from the two different sites. The manuscript text also follows this general structure. Given the size of the plots, some subfigures had to be grouped into separate plots and therefore may not appear strictly in numerical order in the manuscript text.

Comment   Line 217-219: The smaller fraction of Aitken-mode to the total increase may be

caused by a greater accumulation mode contribution. In the summer, we expect to have more SOA in general (stronger emissions of the precursors and stronger oxidation), which also may lead increased organic submicron particle mass

Response We agree with the reviewer that SOA influence may be a viable explanation for the increased accumulation mass contribution, however, our measurement data do not support this.
Changes in SOA concentrations during the daylight hours were small in both seasons (Lee et al., 2015). We also note that accumulation mode particle mass increases were smaller in summer than spring, i.e. even with the likelihood of stronger oxidation conditions in summer the corresponding SOA formation did not seem to lead to significant enhancements in measured organic submicron particle mass.

Comment Line 244-247: The matching of ozone and sulfate is not enough to prove that the nighttime sulfate peak is contributed by heterogeneous SO2 oxidation by ozone. Are there any other evidence?

Response The limited amount of additional measurement data beyond gas-phase standard criteria pollutant data prevents a deeper analysis of this remarkable observation in this work.
We believe that the current wording in the manuscript clarifies that the observed trends are indications ("this points to…") and can serve as impetus for further future study.

Comment Line 273-274: While the median MMD seem showing little change, the mean and 25thn75th percentiles show significant diurnal variations (Figure D2). Why? Also, although in Line 103-105, there is a bit information about the diurnal distributions. Figure D2 would confuse readers a lot by the ranking of the values (meaning that medians were not located between 25th and 75th). It is important to clarify what the median, mean, and 25thn75th stand for? I mean not the median values of MMD values but the MMD from a reconstructed distribution, right?

Response The reviewer's interpretation of the different size distribution groups is correct. We have added an additional Figure 1 in the main text to illustrate the origin of these size distributions to better guide the reader in the discussions following later on. The Figure is appended at the bottom of this document.
In Figure D2, left lower panel for nitrate, there is indeed a notable diurnal variation in the mean set MMD. The 25th and 75th percentile distributions exhibit certain fluctuations, which are however minor and within a narrow range. We further take note of this observation in Lines 293-298, where the differences in distribution sets are discussed. We believe that this difference between the percentile (25th PC, median, 75thPC) sets and the mean set is an effect of averaging same-hour concentration values from different days to yield the diurnal average values. As different days may experience different concentration levels (longer-term fluctuations, e.g. transport, photochemically active periods etc.) and may be distributed disproportionately across certain hours of the day, this results in "skewed" average size distributions. As noted in the manuscript, we therefore chose to utilize median data in this study for the interpretation of diurnal variations.

Alteration Addition of Figure 1 to show the sequence of main data treatment and analysis steps.

Comment Overall the discussion in Section 3 only focused on what were seen from this study. Do the interpretations agree or disagree with what are known from other studies (other than AMS). For example, for mixing state, are the findings here consistent with the understanding from single particle analysis? The paper needs to show which results are novel and which ones have already been published from previous analysis in terms of understanding the sources and atmospheric processing of submicron particles.

Response Size distribution studies in Hong Kong are generally rare and are either not chemically resolved (SMPS, FMPS) or rely on MOUDI sampling.
Comparability is limited, given different sizing techniques (mobility vs. aerodynamic / vacuum-aerodynamic), sampling times (real-time or near-real time vs. 24h to 48h) and aerosol pre-treatment (removal of water for AMS measurements vs. "as-is" for MOUDI and SMPS typically). To our knowledge, single particle analysis from ambient measurements in Hong Kong analyzing particle mixing state have not been reported yet. We have added a section on particle size distribution measurements undertaken in Hong Kong in the revised manuscript.

With respect to novelty, as noted in the introduction, the main focus of this paper is to demonstrate a systematic method of utilizing AMS size distributions and to provide chemically resolved particle mass size distributions on finer temporal scales. Detailed chemically resolved diurnal size distribution variations and longer term daily size distribution measurements from ambient AMS sampling campaigns are scarce, as are detailed size distribution studies focusing on the Hong Kong and Pearl River Delta Region.

Alteration   Addition of Chapter 3.3 in the main text. The relevant part is appended to the bottom of this document.

Comment   Technical remarks: Line 107: Extra period after "the world". Line 157: Add hyphen between "Aitken" and "mode" when used as adjective. Similarly for "accumulation mode particle concentrations" and so on.

Response   We have taken these technical remarks into account in our manuscript revision.

<u>**Changes in sections of main manuscript and Supporting Material**</u>
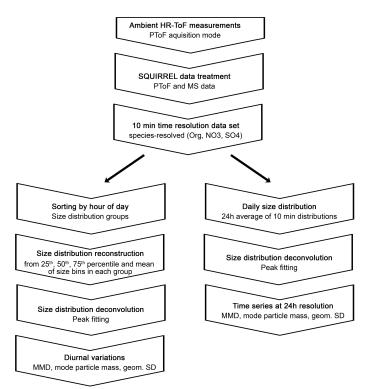<u>**Main manuscript**</u>

```
┌─────────────────────────────┐
│ Ambient HR-ToF measurements │
│    PToF aquisition mode     │
└─────────────────────────────┘
          │
┌─────────────────────────────┐
│   SQUIRREL data treatment   │
│      PToF and MS data       │
└─────────────────────────────┘
          │
┌─────────────────────────────┐
│ 10 min time resolution data set │
│ species-resolved (Org, NO3, SO4) │
└─────────────────────────────┘
        ╱        ╲
┌──────────────────────┐   ┌──────────────────────┐
│  Sorting by hour of day │   │  Daily size distribution │
│ Size distribution groups │   │ 24h average of 10 min distributions │
└──────────────────────┘   └──────────────────────┘
          │                          │
┌──────────────────────┐   ┌──────────────────────┐
│ Size distribution reconstruction │   │ Size distribution deconvolution │
│ from 25th, 50th, 75th percentile and mean │   │          Peak fitting          │
│    of size bins in each group     │   └──────────────────────┘
└──────────────────────┘              │
          │                 ┌──────────────────────┐
┌──────────────────────┐   │ Time series at 24h resolution │
│ Size distribution deconvolution │   │ MMD, mode particle mass, geom. SD │
│          Peak fitting          │   └──────────────────────┘
└──────────────────────┘
          │
┌──────────────────────┐
│   Diurnal variations   │
│ MMD, mode particle mass, geom. SD │
└──────────────────────┘
```

Figure 1. Flow chart of main data acquisition, data treatment and data analysis procedures

[…]

3.3 Comparison to previous studies

Particle size distribution studies in Hong Kong are generally scarce and have focused on either size segregated filter samples (MOUDI) for general ambient measurements or electrostatic classification in particle formation and particle growth studies (Guo et al., 2012;Cheung et al., 2015) . The latter studies focus on specific and narrow time periods and lack general discussions on ambient particle size distributions.

Two ambient studies were undertaken at the suburban coastal HKUST site using size-segregated samples from a ten-stage MOUDI sampler and offline chromatographic analysis. Inorganic constituents (NH4, NO3, SO4) in fine particles (i.e. $D_p<1.8$ µm) were shown to follow bimodal distributions with mode diameters in the range of 0.14-0.21 µm and 0.46-0.58 µm in samples collected in the winter season, while the main mode was observed in the coarse region (4-6 µm) for all three species (Zhuang et al., 1999). A subsequent year-long observational study also reported bimodal fine particle distributions with mode diameters of 0.1-0.3 µm and 0.7–0.9 µm and 1-2 additional modes in the coarse region (Bian et al., 2014), however, the main mode in the size distributions of sulfate, ammonium, potassium and oxalate was observed in the droplet mode (0.7 – 0.9 µm) in this study. Vehicle exhaust plumes sampled on-road from a Mobile Real-time Air Monitoring Platform (MAP) across Hong Kong's road network exhibited three distinct particle volume size distributions: a unimodal distribution with an accumulation mode at 0.2 µm and two bimodal distributions with a minor mode at 0.2 µm and the dominant mode at 0.5 or 0.7 µm (Yao et al., 2007).

The bimodality in the fine particle range across these studies is consistent with the AMS-based results in this work. Nominally, the accumulation mode diameters from filter based studies and the chase studies are larger than those from AMS measurements where maximum mode diameters occurred at D_{va} ~ 700nm, corresponding to D_a ~ 470 (assuming D_{va} ~ D_a * density; particle density ~ 1.5 g/cm^3). Direct comparability is however limited due to

fundamental differences in sizing techniques (MOUDI: atmospheric pressure; AMS: near-vacuum), sampling times (MOUDI: 24h samples, scattered time line; AMS: minute raw resolution averaged to hourly or daily, continuous time line), measurement uncertainties (MOUDI: sampling artifacts such as vapor adsorption and desorption; AMS: inlet lens transmission) and aerosol pretreatment (none for MOUDI with potential impacts on particle size in high humidity (>80%) conditions (Fang et al., 1991); AMS: removal of water prior to introduction to instrument).

Supporting Material

Lognormal peaks were fitted to each 24h and hour-of-day AMS mass size distribution respectively employing the *Multipeak Fit V2* algorithm in *Igor Pro (Wavemetrics)* using a simple vertical offset as the baseline and initial guesses on peak position, height, and width based on visual inspection of the raw size distribution. The multipeak fitting tool employs the Levenberg-Marquardt algorithm (Gill et al., 1981) as a non-linear least squares fit and iteratively adjusts the initial fit parameter guesses until a convergent solution with minimized residuals is achieved. In sporadic cases, the fitted solution led to excessive deviations from the initial guesses with greatly shifted peak locations and large fluctuations in peak width. In such cases, results from the peak fits of immediately adjacent size distributions (i.e. previous and next distributions in the sequence) were evaluated and used to adjust the fitting process by fixing either the location (*primary*) or the width of the peak (*secondary*) to the average value of the two adjacent fitted distributions.

For the diurnal size distributions, measurement data from time periods with large differences in species concentration levels were pooled together. The averaging of mass (or volume) based size distribution involves different uncertainties for each size bin due to the cubic relationship between particle mass (or volume) and particle diameter and the corresponding improvement in signal-to-noise ratio with increasing particle size. To establish reliable diurnal trends, we adopt an approach similar to the analysis of conventional species concentration diurnal trends by evaluating size distributions reconstructed from the average, median, 25th and 75th percentile of each size bin. Similar diurnal trends in the fitting parameters across these different size distributions would confirm that changes were indeed recurrent daily while divergent trends would indicate that irregular processes (e.g. episodic events) were more significant in determining size distribution characteristics. Since episodic pollution events and clean periods (e.g. prolonged precipitation) were not removed from the dataset, the quantitative analysis focuses on trends observed in the median dataset to minimize skewing effects of high and low concentration periods.

Uncertainties can arise from the peak fitting process itself. While the bimodality of the size distributions was obvious in most cases (i.e. a main mode with a shoulder towards smaller particle sizes, e.g. Figure D1), accumulation mode particle mass can occasionally dominate the mass size distribution and diminish the Aitken mode. To achieve confidence in the appropriateness of the bimodal fitting we evaluated both unimodal and bimodal peak fits whenever the Aitken to accumulation mode peak ratio was <10% and we depict a representative example below (Figure D2a. b). The distribution of the fit residuals (Figure D2c, d) was examined and cumulative probability distributions of the fit residuals compared by the Kolmogorov-Smirnov test (Figure D2e) to assess whether fit residuals were significantly different at 95% confidence level (CL). It is evident that the bimodal fit performs better at resolving the raw size distribution in the smaller size region and overall yields a more normal residual distribution. The Kolmogorov-Smirnov test confirms that the residual distributions are statistically different (D>$D_{critical}$ at 95% CL). We tested all borderline cases using the outlined procedure. In this study, bimodal fits yielded unanimously better results in all cases for both diurnal and day-to-day size distributions and all investigated species, i.e. the Aitken mode always remained clearly distinguishable from the accumulation mode.

While the peak fitting algorithm yields a unique individual solution with a set of parameters for which resulting residuals (*difference of fitted and original distribution*) are minimized, the surrounding solution space provides a potentially infinite number of similar solutions with slightly larger residuals. The standard deviations of the fit parameters can provide an estimate of the variability of the peak parameters between the final fit solution and the surrounding solution space. We evaluated the uncertainty in peak area (i.e. integrated mode particle mass) which represents the combined uncertainty of the peak position, width and height (which altogether directly determine the peak area) for all fitted size distributions in this work.

Figure D3 depicts the standard deviation of resolved peak area (i.e. integrated mode particle mass concentration) nominally and relative to the peak area for the diurnal size distributions of NO3 at the urban Mong Kok site in summer 2013 and Tables C1-C2 summarize the values of percent standard deviations for all species at both measurement sites respectively. The median datasets, which were used for quantitative discussion for the diurnal size distribution analysis, exhibited particle mass uncertainties of 14-48% in the Aitken mode and 1-12% in the accumulation mode at the suburban HKUST site, and 7-44% in the Aitken mode and 1-6% in the accumulation

mode at the urban MK site. Figure D4 depicts the 75th percentile-bin diurnal variation of NO3 (which displayed the largest uncertainties in Figure D3) with the corresponding peak area variability, and shows that the interpretation of the diurnal variation would remain largely unaffected from the incurred uncertainties.

For the day-to-day 24h size distributions a corresponding analysis was undertaken, with Figure D5 depicting the size distributions of NO3 at the HKUST site for all covered seasons exemplarily, and Table C3 summarizes the values of percent standard deviations for all species at both measurement sites respectively. Peak fit uncertainties typically increase with decreasing integrated peak area and can exceed the values of the peak area in the Aitken mode in a small number of cases (e.g. Figure D5c,e – ratios >1). Quantification of the Aitken mode may not be possible at high levels of confidence in these isolated cases. They were retained in the dataset due to their low frequency of occurrence and to enable a complete discussion over the full concentration range without biasing towards larger concentration (i.e. fitted peak areas) values.

Table C1. Percentiles of relative standard deviation (*rows; corresponding to the box-whiskers plot in Figure D3e,f*) in percent from lognormal peak fits (bimodal deconvolution) for the resolved Aitken mode (a) and accumulation mode (b) particle concentration for diurnal size distributions at the HKUST supersite (2011/12), *columns* describe the data set, i.e. reconstructed size distributions from the 25th percentile, median, 75th percentile and mean of the size bins
Sp=Spring, Su=Summer, Fa=Fall, Wi=Winter

(a)

Aitken mode % SD		25th PC Distr.				Median Distr.				75th PC Distr.				Mean Distr.				Range
		Sp	Su	Fa	Wi	Sp	Su	Fa	Wi	Sp	Su	Fa	Wi	Sp	Su	Fa	Wi	
NO3 (UST)	PC-90	67	76	39	85	76	44	54	55	80	75	56	39	36	77	44	42	36-85
	PC-75	52	42	28	57	66	32	39	40	61	59	44	29	22	38	35	34	22-66
	PC-50	**36**	**33**	**22**	**46**	**44**	**26**	**31**	**22**	**40**	**43**	**34**	**23**	**18**	**28**	**24**	**30**	**18-46**
	PC-25	29	25	16	28	26	14	24	18	25	29	22	17	14	19	20	25	14-29
	PC-10	21	20	15	24	19	12	19	15	17	19	17	10	13	13	15	21	10-24
SO4 (UST)	PC-90	38	38	42	74	19	36	39	43	22	40	40	42	19	36	37	81	19-81
	PC-75	35	33	38	55	18	28	33	32	18	30	35	64	17	30	30	66	17-66
	PC-50	**28**	**30**	**33**	**32**	**16**	**26**	**27**	**25**	**14**	**24**	**27**	**27**	**14**	**24**	**26**	**48**	**14-48**
	PC-25	21	25	26	24	13	21	22	21	11	18	24	22	12	21	23	40	11-40
	PC-10	17	23	24	19	11	20	20	13	10	14	20	19	10	19	22	35	10-35
Org (UST)	PC-90	52	23	41	44	42	28	32	27	47	48	45	53	46	29	24	32	23-53
	PC-75	41	18	26	28	30	22	27	22	26	39	35	44	36	23	21	25	18-44
	PC-50	**26**	**14**	**17**	**21**	**19**	**18**	**21**	**17**	**20**	**32**	**26**	**35**	**23**	**18**	**19**	**21**	**14-35**
	PC-25	16	11	13	18	17	16	19	15	18	28	20	29	18	14	16	17	11-29
	PC-10	9	9	10	11	14	9	15	12	15	20	17	21	17	11	14	16	9-21

(b)

Accum. mode % SD		25th PC Distr.				Median Distr.				75th PC Distr.				Mean Distr.				Range
		Sp	Su	Fa	Wi	Sp	Su	Fa	Wi	Sp	Su	Fa	Wi	Sp	Su	Fa	Wi	
NO3 (UST)	PC-90	8	5	8	4	7	5	6	3	4	9	6	3	3	4	5	1	1-9
	PC-75	6	4	7	3	3	4	5	2	4	7	5	2	2	3	5	1	1-7
	PC-50	**4**	**3**	**5**	**2**	**3**	**3**	**5**	**2**	**3**	**4**	**5**	**2**	**2**	**3**	**4**	**1**	**1-5**
	PC-25	3	3	4	2	2	3	4	1	3	3	4	2	2	2	4	1	1-4
	PC-10	2	2	4	1	2	2	4	1	2	2	3	1	2	2	3	1	1-4
SO4 (UST)	PC-90	2	3	3	5	2	2	2	3	3	2	3	4	2	2	2	2	2-5
	PC-75	2	2	2	2	2	2	2	2	2	2	2	3	1	2	2	2	1-3
	PC-50	**2**	**2**	**2**	**1**	**2**	**2**	**2**	**2**	**2**	**2**	**2**	**2**	**1**	**2**	**2**	**1**	**1-2**
	PC-25	2	2	2	1	1	2	2	1	1	2	2	2	1	2	2	1	1-2
	PC-10	1	2	1	1	1	2	2	1	1	1	2	1	1	2	2	1	1-2
Org (UST)	PC-90	29	12	16	9	18	8	9	5	10	6	7	3	18	7	5	5	3-29
	PC-75	18	9	11	7	10	5	5	3	6	4	5	2	11	5	4	3	2-18
	PC-50	**12**	**7**	**5**	**5**	**6**	**4**	**4**	**3**	**4**	**3**	**4**	**2**	**7**	**3**	**3**	**3**	**2-12**
	PC-25	7	4	3	3	5	3	3	2	3	2	3	2	5	2	2	2	2-7
	PC-10	4	4	1	2	4	2	2	1	2	2	2	1	2	1	2	2	1-4

Table C2. Percentiles of relative standard deviation (*rows; corresponding to the box-whiskers plot in Figure D3e,f*) in percent from lognormal peak fits (bimodal deconvolution) for the resolved Aitken mode (a) and accumulation mode (b) particle concentration for diurnal size distributions at the urban MK site (2013), *columns* describe the data set, i.e. reconstructed size distributions from the 25th percentile, median, 75th percentile and mean of the size bins *Sp=Spring, Su=Summer*

(a)

Aitken mode % SD		25th PC Distr. Sp	25th PC Distr. Su	Median Distr. Sp	Median Distr. Su	75th PC Distr. Sp	75th PC Distr. Su	Mean Distr. Sp	Mean Distr. Su	Range
NO3 (MK)	PC-90	38	46	40	34	40	41	22	26	22-46
	PC-75	27	34	26	28	34	35	20	16	16-35
	PC-50	**15**	**24**	**23**	**21**	**25**	**28**	**18**	**14**	**14-28**
	PC-25	9	20	19	17	18	22	15	12	9-22
	PC-10	6	19	16	14	15	20	13	11	6-20
SO4 (MK)	PC-90	63	46	35	38	24	31	23	21	21-63
	PC-75	50	36	30	36	21	28	21	20	20-50
	PC-50	**44**	**33**	**28**	**24**	**20**	**23**	**19**	**18**	**18-44**
	PC-25	37	27	24	21	17	20	15	17	15-37
	PC-10	33	25	21	19	15	18	15	16	15-33
Org (MK)	PC-90	22	12	22	19	30	21	15	14	12-30
	PC-75	16	10	12	12	18	11	12	8	8-18
	PC-50	**10**	**8**	**10**	**9**	**10**	**9**	**8**	**7**	**7-10**
	PC-25	8	7	8	7	7	8	6	6	6-8
	PC-10	7	6	7	6	6	6	5	5	5-7

(b)

Accum. mode % SD		25th PC Distr. Sp	25th PC Distr. Su	Median Distr. Sp	Median Distr. Su	75th PC Distr. Sp	75th PC Distr. Su	Mean Distr. Sp	Mean Distr. Su	Range
NO3 (MK)	PC-90	9	9	6	7	3	5	2	5	2-9
	PC-75	6	8	4	5	3	4	2	4	2-8
	PC-50	**4**	**6**	**3**	**4**	**2**	**3**	**2**	**3**	**2-6**
	PC-25	2	5	2	4	2	3	1	3	1-5
	PC-10	2	4	1	3	1	3	1	2	1-4
SO4 (MK)	PC-90	4	3	2	3	2	5	2	3	2-5
	PC-75	3	2	2	3	2	4	2	2	2-4
	PC-50	**3**	**2**	**2**	**2**	**1**	**4**	**2**	**2**	**1-4**
	PC-25	2	2	2	2	1	3	1	2	1-3
	PC-10	2	2	1	2	1	3	1	2	1-3
Org (MK)	PC-90	9	8	8	7	9	5	6	6	5-9
	PC-75	6	7	5	5	5	4	5	4	4-7
	PC-50	**5**	**5**	**4**	**4**	**3**	**4**	**3**	**4**	**3-5**
	PC-25	4	4	3	3	3	3	3	3	3-4
	PC-10	2	3	3	3	5	2	2	2	2-3

Table C3. Percentiles of percent standard deviation (*rows; corresponding to the box-whiskers plot in Figure D5e,f*) from lognormal peak fits (bimodal deconvolution) for the resolved Aitken mode and accumulation mode for 24h day-to-day size distributions at the suburban HKUST site (a) and the urban MK site (b) for all investigated species, *columns* describe the uncertainties in terms of quartiles of resolved peak area, where Q1 refers to the lowest 25% and Q4 the highest 25% of resolved peak area (see also Figure D4)

(a)

HKUST '11/12 % SD		NO3					SO4					Org				
		Q1	Q2	Q3	Q4	Range	Q1	Q2	Q3	Q4	Range	Q1	Q2	Q3	Q4	Range
Aitken mode	PC-90	95	64	50	27	27-95	97	78	49	30	30-97	62	37	28	26	26-62
	PC-75	58	47	37	24	24-58	91	57	36	20	20-91	41	24	21	22	21-41
	PC-50	**47**	**35**	**25**	**17**	**17-47**	**60**	**39**	**29**	**16**	**16-60**	**30**	**17**	**14**	**17**	**14-30**
	PC-25	30	25	20	13	13-30	32	26	21	13	13-32	25	14	10	12	10-25
	PC-10	20	16	15	8	8-20	24	18	13	11	11-24	16	11	6	7	6-16
Accum. mode	PC-90	31	9	7	4	4-31	4	3	3	3	3-4	18	11	9	7	7-18
	PC-75	13	6	5	3	3-13	3	3	3	2	2-3	9	7	6	5	5-9
	PC-50	**8**	**4**	**3**	**2**	**2-8**	**2**	**2**	**2**	**2**	**~2**	**6**	**4**	**5**	**3**	**3-6**
	PC-25	3	3	2	2	2-3	2	2	2	2	~2	4	3	3	2	2-4
	PC-10	1	2	2	1	1-2	2	2	2	1	1-2	3	2	2	2	2-3

(b)

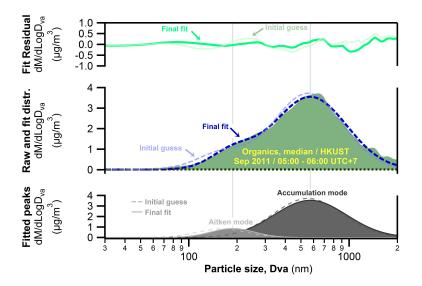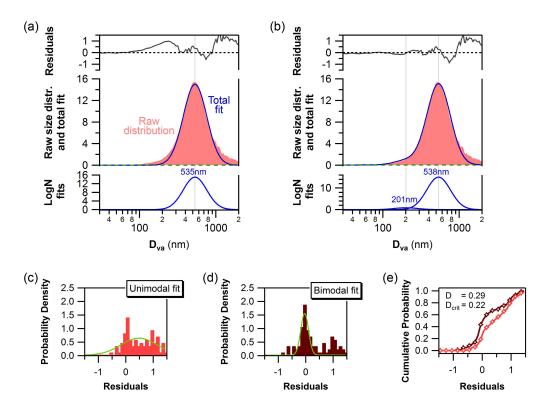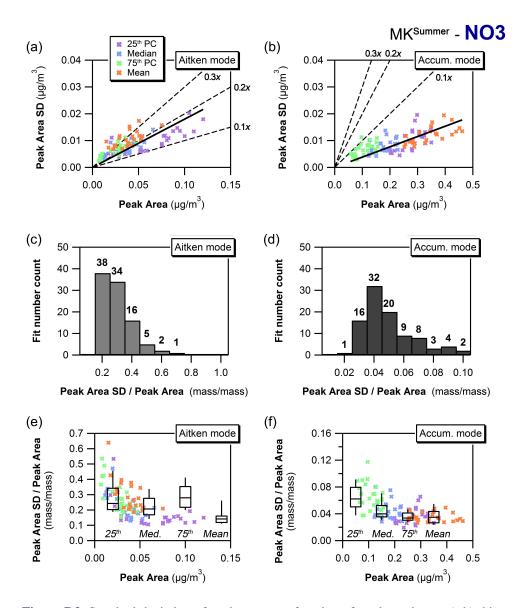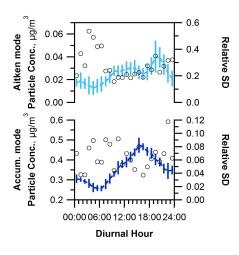| MK '13 % SD		NO3					SO4					Org				
		Q1	Q2	Q3	Q4	Range	Q1	Q2	Q3	Q4	Range	Q1	Q2	Q3	Q4	Range
Aitken mode	PC-90	62	52	47	30	30-62	94	50	29	24	24-94	23	17	13	16	13-23
	PC-75	41	42	30	25	25-42	47	35	22	16	16-47	16	14	11	12	11-16
	PC-50	**28**	**34**	**21**	**18**	**18-34**	**33**	**24**	**17**	**12**	**12-33**	**11**	**10**	**6**	**8**	**6-11**
	PC-25	21	22	19	12	12-22	26	17	13	9	9-26	8	7	5	6	5-8
	PC-10	6	10	13	8	6-13	19	14	10	5	5-19	6	5	3	3	3-6
Accum. mode	PC-90	22	21	6	6	6-22	7	6	6	4	4-7	13	8	9	8	8-13
	PC-75	17	10	5	3	3-17	4	4	4	2	2-4	8	7	6	4	4-8
	PC-50	**10**	**6**	**4**	**2**	**2-10**	**3**	**2**	**2**	**1**	**1-3**	**6**	**5**	**4**	**2**	**2-6**
	PC-25	6	3	2	2	2-6	2	2	1	1	1-2	4	4	3	2	2-4
	PC-10	3	1	2	1	1-3	1	1	1	1	~1	2	3	2	1	1-3

Figure D1. Example of a log-normal peak fit *(Multipeak Fit V2, Igor Pro, Wavemetrics, Levenberg-Marquardt algorithm)* of an AMS organics size distribution
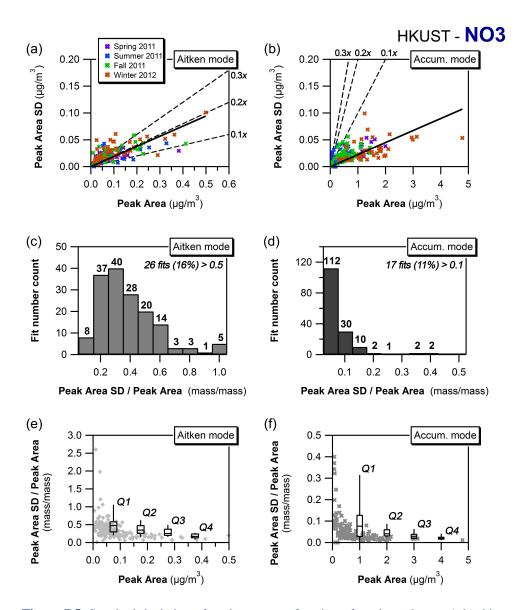

Figure D2. 24h average size distribution of sulfate (12/12/2011, suburban HKUST site) with (a) unimodal and (b) bimodal logN peak fitting applied; histograms of residuals from the unimodal (c) and bimodal (d) distributions with Gaussian fit (green); and cumulative probability density functions of uni- and bimodal fit residuals (e) with Kolmogorov-Smirnov D metric values at 95% confidence level

Figure D3. Standard deviation of peak area as a function of mode peak area (a,b), histogram of relative standard deviation i.e. the ratio of standard deviation to mode peak area (c,d) where the last bin also contains all values beyond the last bin range, and relative standard deviation as a function of mode peak area (e,f) for the fitted Aitken and accumulation mode with binned box-whiskers plot (25th to 75th PC box with horizontal median line and 10th to 90th PC whiskers where bins refer to quartiles of peak area from lowest Q1 to highest Q4); data for diurnal size distributions of NO3 at the urban Mong Kok site in summer 2013.

Figure D4. Plot of 75th percentile-bin diurnal variation with peak area fit variability and relative standard deviation (corresponding to green data and second to last box in Figure D3e,f)

Figure D5. Standard deviation of peak area as a function of mode peak area (a,b), histogram of relative standard deviation i.e. the ratio of standard deviation to mode peak area (c,d) where the last bin also contains all values beyond the last bin range, and relative standard deviation as a function of mode peak area (e,f) for the fitted Aitken and accumulation mode with binned box-whiskers plot (25th to 75th PC box with horizontal median line and 10th to 90th PC whiskers where bins refer to quartiles of peak area from lowest Q1 to highest Q4); data for day-to-day size distributions of NO3 at the HKUST site including all seasons.

References

Bahreini, R., Dunlea, E. J., Matthew, B. M., Simons, C., Docherty, K. S., DeCarlo, P. F., Jimenez, J. L., Brock, C. A., and Middlebrook, A. M.: Design and Operation of a Pressure-Controlled Inlet for Airborne Sampling with an Aerodynamic Aerosol Lens, Aerosol Science and Technology, 42, 465-471, 10.1080/02786820802178514, 2008.

Bian, Q., Huang, X. H. H., and Yu, J. Z.: One-year observations of size distribution characteristics of major aerosol constituents at a coastal receptor site in Hong Kong – Part 1: Inorganic ions and oxalate, Atmos. Chem. Phys., 14, 9013-9027, 10.5194/acp-14-9013-2014, 2014.

Cheung, K., Ling, Z. H., Wang, D. W., Wang, Y., Guo, H., Lee, B., Li, Y. J., and Chan, C. K.: Characterization and source identification of sub-micron particles at the HKUST Supersite in Hong Kong, Science of The Total Environment, 527–528, 287-296, http://dx.doi.org/10.1016/j.scitotenv.2015.04.087, 2015.

Fang, C. P., McMurry, P. H., Marple, V. A., and Rubow, K. L.: Effect of Flow-induced Relative Humidity Changes on Size Cuts for Sulfuric Acid Droplets in the Microorifice Uniform Deposit Impactor (MOUDI), Aerosol Science and Technology, 14, 266-277, 10.1080/02786829108959489, 1991.

Gill, P. E., Murray, W., and Wright, M. H.: The Levenberg-Marquardt method, in: Practical optimization, Academic Press, London, 1981.

Guo, H., Wang, D. W., Cheung, K., Ling, Z. H., Chan, C. K., and Yao, X. H.: Observation of aerosol size distribution and new particle formation at a mountain site in subtropical Hong Kong, Atmos. Chem. Phys., 12, 9923-9939, 10.5194/acp-12-9923-2012, 2012.

Lee, B. P., Li, Y. J., Yu, J. Z., Louie, P. K. K., and Chan, C. K.: Characteristics of submicron particulate matter at the urban roadside in downtown Hong Kong—Overview of 4 months of continuous high-resolution aerosol mass spectrometer measurements, Journal of Geophysical Research: Atmospheres, 120, 7040-7058, 10.1002/2015JD023311, 2015.

Liu, P. S. K., Deng, R., Smith, K. A., Williams, L. R., Jayne, J. T., Canagaratna, M. R., Moore, K., Onasch, T. B., Worsnop, D. R., and Deshler, T.: Transmission efficiency of an aerodynamic focusing lens system: Comparison of model calculations and laboratory measurements for the Aerodyne Aerosol Mass Spectrometer, Aerosol Science and Technology, 41, 721-733, 10.1080/02786820701422278, 2007.

Takegawa, N., Miyakawa, T., Watanabe, M., Kondo, Y., Miyazaki, Y., Han, S., Zhao, Y., van Pinxteren, D., Bruggemann, E., Gnauk, T., Herrmann, H., Xiao, R., Deng, Z., Hu, M., Zhu, T., and Zhang, Y.: Performance of an Aerodyne Aerosol Mass Spectrometer (AMS) during Intensive Campaigns in China in the Summer of 2006, Aerosol Science and Technology, 43, 189-204, 10.1080/02786820802582251, 2009.

Williams, L. R., Gonzalez, L. A., Peck, J., Trimborn, D., McInnis, J., Farrar, M. R., Moore, K. D., Jayne, J. T., Robinson, W. A., Lewis, D. K., Onasch, T. B., Canagaratna, M. R., Trimborn, A., Timko, M. T., Magoon, G., Deng, R., Tang, D., de la Rosa Blanco, E., Prévôt, A. S. H., Smith, K. A., and Worsnop, D. R.: Characterization of an aerodynamic lens for transmitting particles greater than 1 micrometer in diameter into the Aerodyne aerosol mass spectrometer, Atmos. Meas. Tech., 6, 3271-3280, 10.5194/amt-6-3271-2013, 2013.

Yao, X., Lau, N. T., Chan, C. K., and Fang, M.: Size distributions and condensation growth of submicron particles in on-road vehicle plumes in Hong Kong, Atmospheric Environment, 41, 3328-3338, 10.1016/j.atmosenv.2006.12.044, 2007.

Zhang, Q., Stanier, C. O., Canagaratna, M. R., Jayne, J. T., Worsnop, D. R., Pandis, S. N., and Jimenez, J. L.: Insights into the chemistry of new particle formation and growth events in Pittsburgh based on aerosol mass spectrometry, Environmental Science & Technology, 38, 4797-4809, 10.1021/es035417u, 2004.

Zhuang, H., Chan, C. K., Fang, M., and Wexler, A. S.: Size distributions of particulate sulfate, nitrate, and ammonium at a coastal site in Hong Kong, Atmospheric Environment, 33, 843-853, 10.1016/s1352-2310(98)00305-7, 1999.